Journal of Engineering and Applied Sciences 13 (23): 9914-9923, 2018
ISSN: 1816-949X

Mechanical Properties and Bacterial Adhesion of Anatase Nanoparticles Reinforced Poly (Methyl Methacrylate)

[1]Imad Ali Disher Al-Hydary and [2]Muna Sabbar Jebar Al-Rubiae
[1]Department of Ceramics and Building Materials, College of Materials Engineering, University of Babylon, Hillah, Iraq
[2]Babylon Technical Institute, Department of Medical Analysis, Al-Furat Al-Awsat Technical University, Babylon, Iraq

Abstract: In the present research, anatase nanoparticles as reinforcement and bacterial adhesion reducer were incorporated into a matrix of poly (methyl methacrylate) to obtain a composite material which combines adequate mechanical properties and high resistance to bacterial adhesion. The common pathological bacterial species, *Pseudomonas aeruginosa*, *Staphylococcus aureus* and *Klebsiella pneumonia* were selected for the bacterial adhesion tests. The surface properties of the composites were investigated and correlated to the adhesion behavior using nonlinear regression technique. The results showed that anatase nanoparticles improve the stiffness and the compressive strength of the PMMA matrix, however, the flexural strength is reduced noticeably. Nevertheless, a composite containing 10 wt.% of the anatase nanoparticles has the highest resistance to the bacterial adhesion and adequate flexural strength. Moreover, the regression analysis produced a common nonlinear model which excellently fits the experimental data for the different bacterial species using the contact angle, the nanoscale roughness and the microscale roughness as independent variables.

Key words: Anatase, bacterial adhesion, PMMA polymer, polymer composites, nanoparticles, experimental

INTRODUCTION

The adhesion of the bacteria to the surfaces of solids has great impact in the environmental, medical and industrial applications. Thus, for many decades, it attracted extensive interest from many researchers. Although, the bacterial adhesion is very important for many beneficial microbial communities, it is the first step for the colonization of pathogenic bacteria that causes many diseases and fouling in many environments and industries (Xing *et al*., 2015; Guegan *et al*., 2014; An and Friedman, 1998).

Different strategies have been developed to prevent or reduce the adhesion of the undesired bacteria to the surfaces and hence, prevent the subsequent biofilm formation. These strategies typically include the use of the biocides (Schaechter, 2004; Li and Ye, 2015), the antibacterial metallic ions (Sharmila *et al*., 2017; Chaw *et al*., 2005; Furno *et al*., 2004), the highly reactive species produced by the photocatalysts (An and Friedman, 1998; Lorenzetti *et al*., 2015) and recently the superhydrophobic surfaces (Zhang *et al*., 2013; Gu and Ren, 2014; Hasan *et al*., 2018). However, drawbacks are associated with the use of biocides and antibacterial metallic ions. These mainly include the increase of the bacterial resistance and cross-resistance to antibiotics due to the use of biocides (Hasan *et al*., 2018; Rodrigues, 2011; Gu *et al*., 2016) and the potential implications for human health and environment due to the use of metallic ions such as Ag^+ ion (Lorenzetti *et al*., 2015; Han *et al*., 2016; Singh *et al*., 2015). Based on that incorporating the surface with photocatalysts and superhydrophobic particles became an important research area in the last few years (Hasan *et al*., 2018). However, understanding the phenomena associated with the bacterial adhesions to these surfaces and their inhibitions are still under development (Razatos *et al*., 1998; Torres *et al*., 2005; Li and Logan, 2004).

Anatase which is the stable phase of TiO_2 at law temperatures is a proved candidate to resist the bacterial adhesion. It has a photocatalytic activity higher than that of the common TiO_2 rutile phase (Singh *et al*., 2015; He *et al*., 2013; Puckett *et al*., 2010; Giordano *et al*., 2011). Thus, it has the ability to produce different reactive species, such as hydroxyl radical, hydrogen peroxide and superoxide in different environments. Moreover, anatase nanoparticles have been reported to have superhydrophobic characteristics. That is why anatase

Corresponding Author: Imad Ali Disher Al-Hydary, Department of Ceramics and Building Materials, College of Materials Engineering, University of Babylon, Hillah, Iraq

nanoparticles and nanostructures attracted considerable interest in reducing the bacterial adhesion to surfaces (He *et al*., 2013; Jiang *et al*., 2009).

Though, the fragile structure and the fast degradation of the surface chemistry of the nanomaterials hinder their applying in real applications. In order to deal with this issue, many routes are still in early development stages, however, the use of composite materials is the most mature route for facilitating nanoparticles durably for inhibition bacterial adhesion (Guegan *et al*., 2014; Hasan *et al*., 2018; Pavithra and Doble, 2008). Unfortunately while the high percent of nanoparticles in the composites is necessary for the reduction of the bacterial adhesion, it results in serious declineinthe mechanical properties. This is mainly due to the agglomeration of the nanoparticles and the formation of voids in the composites (Crosby and Lee, 2007).

In our previous research, phase pure anatase nanoparticles were prepared and incorporated ina matrix of Poly Methyl Methacrylate (PMMA) with high weight percents (Al-Rubiae, 2016). The bacterial adhesion test gave evidences that these composites have the ability to reduce the bacterial adhesion noticeably. In the current research, the effect of the high weight percents of the anatase nanoparticles on the mechanical properties of TiO_2/PMMA composites was investigated.

Moreover, in the current research, the nonlinear regression technique was adopted for the first time as per our best knowledge to correlate the number of adhering bacteria to the surface properties of the composites. Many research works have been reported to correlate the adhesion of the bacteria to the surface properties of the bacteria as well as the substratum using different approaches (Donlan, 2002; Cheng *et al*., 2007; Wassmann *et al*., 2017; Habash and Reid, 1999). Correlating the material properties to the adhering bacteria is very important because the mechanisms underlying the adhesion of bacteria to the surface are still unclear (Song *et al*., 2015; Habimana *et al*., 2014; Speranza *et al*., 2004). However, the improper selection of the variables and the regression technique led to poor agreement between the model and the experimental data. For example, many studies included the surface free energy, polarity of the surface and the work of adhesion as independent variables in their models, although, these are dependant variables of the contact angle which is already included in the models as independent variable (Donlan, 2002; Habash and Reid, 1999; Teughels *et al*., 2006; Tanner *et al*., 2005; Quirynen *et al*., 1990). This indicates that better models are still needed. In the current research, the number of adhering bacteria was selected as dependant variable while the contact angle, nanoscale roughness and the microscale roughness were selected as independent variables because the surface roughness and the hydrophobicity are the main factors influencing microbial adhesion (Hasan *et al*., 2018; Rochford *et al*., 2014).

MATERIALS AND METHODS

Poly (Methyl Methacrylate) from (Acros, M.W. 35000) and acetone from (Sigma-Aldrich, NLT 99.5%) were used as received without further treatments. TiO_2 nanoparticles were prepared as described in our previous research (Al-Hydary, 2014). The particle size of these nanoparticles is in the range of 30-70 nm and the BET surface area is 38 m^2/g.

Different TiO_2 weight percents of 1, 5, 10, 20 and 35 were used to prepare the TiO_2/PMMA composites. The composites were prepared by mixing two mixtures; The first is a PMMA solution in acetone and the second is a suspension of TiO_2 nanoparticles in acetone. The polymer solution was prepared by dissolving the PMMA in acetone with a ratio of 1g of the polymer per 7 mL of acetone at 50°C under magnetic stirring. While the suspension was prepared by mixing the TiO_2 nanoparticles with acetone with a ratio of 1g of TiO_2 nanoparticles per 20 mL of acetone at room temperature using sonication treatment for 2 h. The suspension was added to the solution and the resulting mixture was aged at room temperature under magnetically stirring overnight. After aging, a paste like material was obtained by adding distilled water drop wise to the mixture with continuous stirring. The paste was oven-dried at 80°C for 24 h and crashed using mortar and pestle to form granules.

Hotpressing method was used to form the prepared granules into pellets using a steel die and hydraulic press with controlled heating unit. The specimens were heated up to 155°C under a pressure of 11 MPa using a heating rate of 2°C/min. After that the specimens were allowed to cool to room temperature while the applied pressure was maintained. The specimens were cut to the desired dimensions and subjected to ordinary surface grinding process using SiC-paper from 600-1200 grit and were polishedusing alumina powder with average particle size of 1, 0.3 and 0.05 μm.

FTIR test was performed for the TiO_2 nanoparticles and PMMA polymer as well as their composites to study the bonding between the matrix and the reinforcement. The FTIR spectra were recorded using (Shimadzu 1800, Japan) over wavenumber range of 400-4000 cm^{-1} with a resolution of 2 cm^{-1}.

The density of the specimens was measured using Mettler Toledo (AG204, Switzland) densitometer and the

theoretical density was estimated using the mixing rule. The results were used for the comparison between the measured and estimated density to have an idea about the defects in the structure of the composites.

A universal test machine (Instron 5500R, USA) was used to measure the ultimate-point compressive and flexural strengthsusing 150 kN load cell at a crosshead speed of 0.5 mm/min.The R scale Rockwell Hardness (RHR) wastested usingdigital hardness testers (TRSD M/P, India).

Automated contact angle instrument (SL200K series, KINO) was used to measure the contact angle of the samples using the sessile drop technique and deionized water at 25°C. The measurements, for triplicate samples, were achieved within 15 sec after the positioning of automatically dropped 3 μL droplet. The Surface Free Energy (SFE) was calculated based on the average contact angle data using the Neumann's standard formula.

The microscale surface roughness was measured at three different sites with a stylus instrument (SRT-6210) for three specimens of each composite. The micro roughness values were given as arithmetic average peak-to-valley value (μRa).

The 3D images of the surface topography were obtained from a scan probe microscope machine (SPM-AA3000, Angstrom Advanced, USA) using the tapping mode scan, this method was also used to determine the surface nanoroughness at randomly selected areas of (10×10 μm) of each specimen.

The culture of *Pseudomonas aeruginosa (PA), Staphylococcus aureus (SA)* and *Klebsiella pneumonia (KP)* bacterial species and their adhesion tothe sterilized specimens were performed as described in our previous research given in details else where (Al-Rubiae, 2016).

Minitab Software (17.3.1) was used to analyze the obtained data and to perform the nonlinear regression; Also, OriginPro 2016 Software (b9.3.266) was used to represent the results graphically.

RESULTS AND DISCUSSION

The FTIR spectraof the anatase nanoparticles, PMMA polymer and TiO_2/PMMA composite are shown in Fig. 1. For the anatase nanoparticles, two bands at 500-800 and 1033 cm^{-1} assigned to Ti-O vibration have been noticed (Busani and Devine, 2005; Nakamoto, 2009). For the PMMA polymer, the bands assigned to asymmetric and symmetric CH_2 stretching vibrations were observed at 2958 and 2933 cm^{-1}. The bands attributed to ester methyl stretching vibrations were noticed at

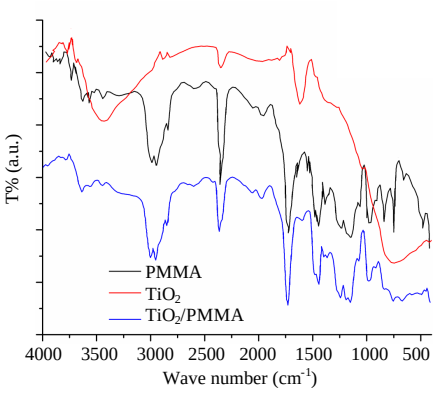

Fig. 1: FTIR spectra of PMMA polymer, anatase nanoparticles and TiO_2/PMMA composite

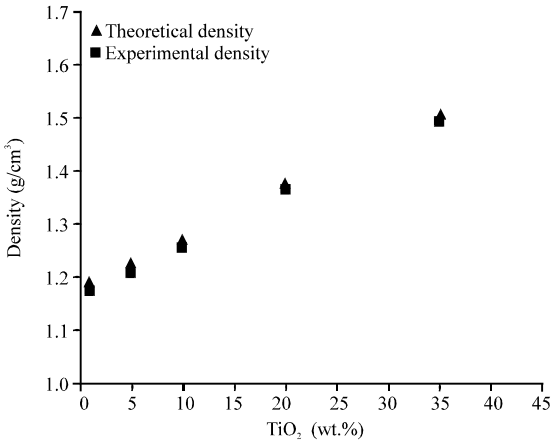

Fig. 2: The experimental and the theoretical density of the TiO_2/PMMA composites

2995, 2948 and 3025 cm^{-1}. The band at 1733 cm^{-1} is arising from carbonyl vibration. The broad peak ranging from 1260-1000 cm^{-1} is owing to the C-O stretching vibration of ester bond. The band at 950-650 cm^{-1} is due to the bending of C-H (Lipschitz, 1982; Balamurugan *et al*., 2004). In the FTIR spectrum of the anatase (20 wt.%) PMMA composite, the PMMA peaks at 1520-1560, 1640 and 3720 cm^{-1} and the anatase band at 1033 were almost disappeared and most of the PMMA peaks were subjected to shifting and variation in the intensities in the spectrum of the composites while new peaks at 590, 1600, 1440 and 2460 cm^{-1} have been observed in the spectrum of the composites. These changes indicatethe interaction between the anatase nanoparticles and the PMMA groups.

Figure 2 shows a comparison between the experimental and the theoretical density which was calculated according to mixing rule of the anatase/PMMA composites. It can be seen that there is a noticeable

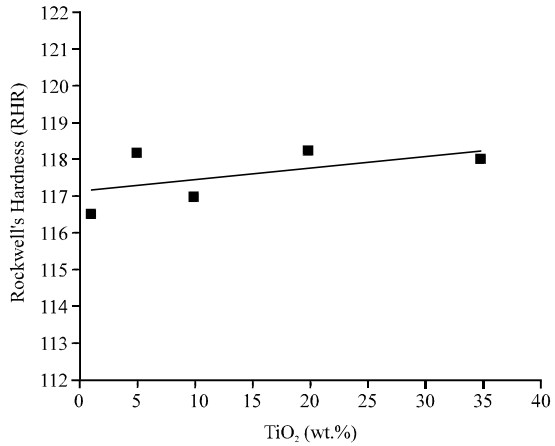

Fig. 3: Rockwell's hardness of the TiO_2/PMMA composites

matching between the two densities of the composites. This suggests the potential of the followed preparation method to produce a sound compositeas compared with the traditional melt mixing or solution casting methods. This implies that the followed method can overcome one of the main challenges in the preparation of polymer matrix composites; Namely the ability to increase the level of nano reinforcement which is not only important for mechanical properties but also for the other properties (Crosby and Lee, 2007). However, minor deviation of <1.1% of the theoretical density could be noticed indicating the development of minor defects in the structure of the composites. These defects may be developed because of the agglomeration of the anatase nanoparticles.

Rockwell's hardness of the prepared composites is shown in Fig. 3. As a general trend, the hardness of the composites increases with the increment of TiO_2 percentage, this indicates the reinforcement role of TiO_2 nanoparticles in the matrix of PMMA polymer. This role is clearly appeared in the compressive strength of the TiO_2/PMMA composites shown in Fig. 4. However, when the TiO_2 percentage exceeds 10 wt.%, a gradual decrement in the strength can be noticed may be due to the agglomeration defects. These defects seem to dominate the mechanical behavior of the composites in the case of flexural strength as shown in Fig. 5 because the flexural strength is very sensitive to the defects in the structure as compared with the compressive strength.

The compressive and flexural moduli of elasticity of the TiO_2/PMMA composites are shown in Fig. 6 and Fig. 7, respectively. It can be seen that the stiffness of the composites enhances with increasing the TiO_2 percent, this is due to the hindering the movement of the polymer chains as a result of the reinforcement role of TiO_2.

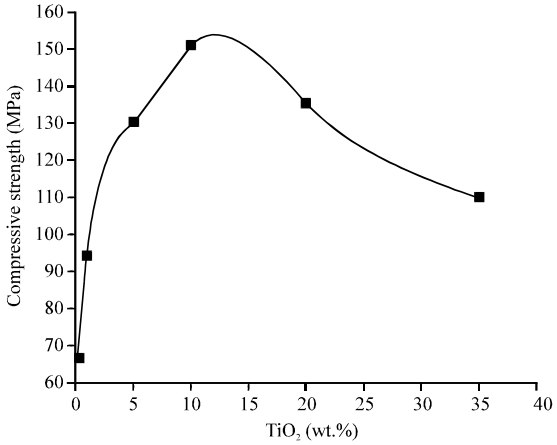

Fig. 4: The compressive strength of the TiO_2/PMMA composites

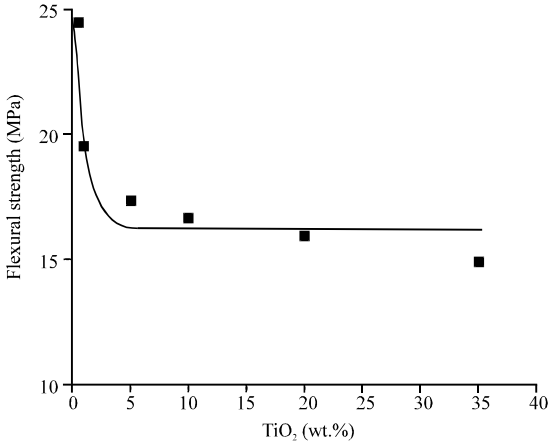

Fig. 5: The flexural strength of the TiO_2/PMMA composites

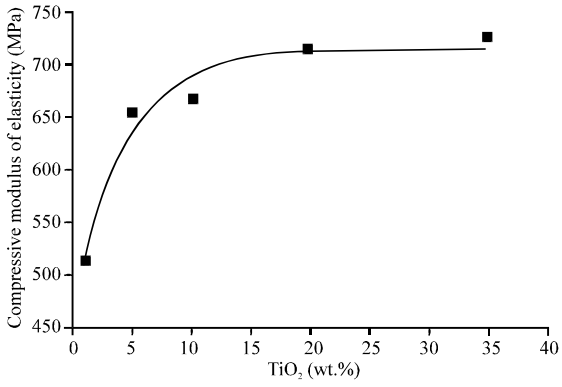

Fig. 6: The compressive modulus of elasticity of the TiO_2/PMMA composites

Figure 8 demonstrates the contact angles of the prepared composites. As illustrated in Fig. 9, the contact angle value increases rapidly when the TiO_2 nanoparticles

are incorporated in PMMA matrix and the surface of the composite becomes hydrophobic with contact angle higher than 90° when the amount of TiO_2 exceeds around 3 wt.%. This is expected because of the high hydrophobicity of the anatase nanoparticles. This indicates the weak interaction between the water and the hydrophobic surface of the composites as shown in Fig. 10 which illustrates the values of the Surface Free Energy (SFE) of the composites.

The three dimensional topographic images of the composites are shown in Fig. 11. It can be seen that the nanoscale features of the surface become finer and shallower for some extent, upon the addition of anatase nanoparticles, these features work on trapping air bubbles and reduce the contact with water (Hasan *et al*., 2018; Belaabed *et al*., 2016). The nanoscale topographical features and the weak chemical interaction explain the hydrophobic nature of the surface. Moreover, these features produced a nanoscale Roughness (nRa) that is reduced upon the addition of the anatase nanoparticles as given in Table 1. On the other hand, the variation in the machineability of the composites produced a fluctuating microscale Roughness (μRa) as given in Table 1.

The numbers of the adhering bacteria to the surface of the TiO_2/PMMA composites are given in Table 2. It is obvious that the number of adhering bacteria is reduced when the TiO_2 nanoparticles is incorporated in the PMMA polymer regardless the type of the selected pathological bacterial species. Also, it is clear that the linear regression isn't a suitable to correlate the values of the selected independent variables and the numbers of adhering bacteria. Based on that the nonlinear regression technique was used to correlate the obtained data. The regression showed that for all the selected pathological

Table 1: Values of the contact angle, nanoroughness and microroughness of the TiO_2/PMMA composites

TiO_2 (wt.%)	Contact angle (°)	Nanoroughness nRa (nm)	Microroughness μRa (μm)
1	73.29	6.39	2.07
2	84.48	3.33	0.84
5	98.58	0.97	1.22
10	99.54	1.29	0.45
20	101.97	1.50	0.79
35	102.04	1.69	1.75

Table 2: Number of adhering bacteria on the TiO_2/PMMA composites

	Number of adhering bacteria		
TiO_2 (wt.%)	*Staphylococcus aureus* (SA)	*Pseudomonas aeruginosa* (PA)	*Klebsiella pneumonia*(KP)
0	211769	1274935	54023
1	73641	797462	18696
5	88739	616241	8479
10	57754	505347	8049
20	55673	671784	9464
35	63013	685261	9058

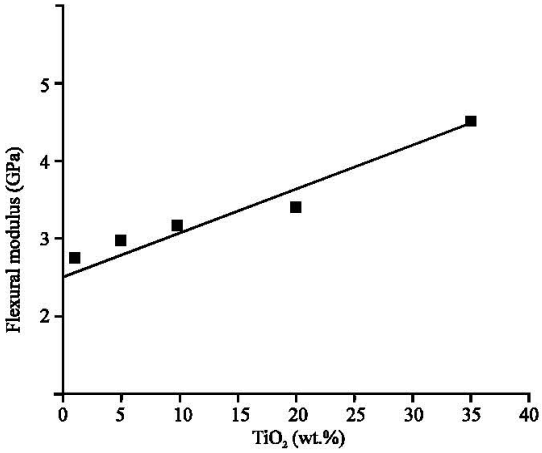

Fig. 7: The flexural modulus of elasticity of the TiO_2/PMMA composites

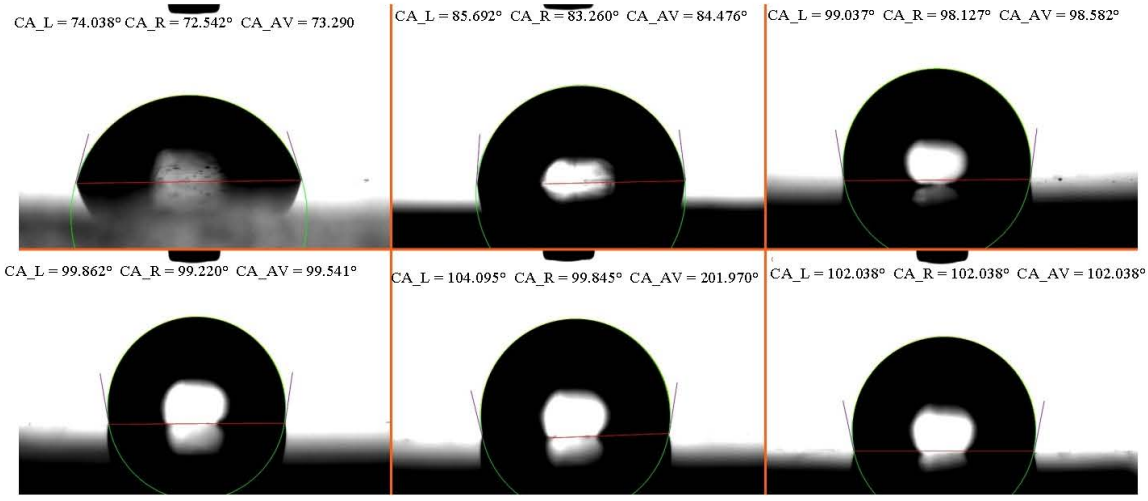

Fig. 8: The images of the sessile water drop on the surface of TiO_2/PMMA composites

bacterial species, there is a common form for the fitting equation that correlates the selected independent variables with the number of the adhering bacteria, the form of that equation is given in Eq. 1:

$$D = C_1+C_2X_1+C_3X_2+C_4X_1X_2+C_5X_1X_3+C_6X_2X_3 \quad (1)$$

Where:

D = The number of adhering bacteria
X_1 = The contact angle
X_2 = The nanoscale Roughness (nRa)
X_3 = The microscale Roughness (μRa)

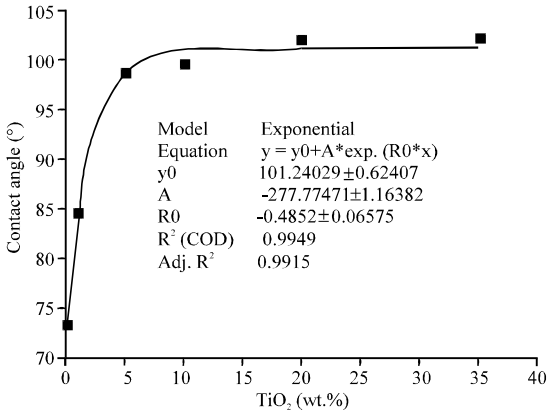

Fig. 9: The contact angles of the TiO_2/PMMA composites

C_i are the coefficients of the equation which depend on the type of the species and find the relative importance of the variables in the adhering process. The values of these coefficients are given in Table 3 along with the values of the coefficient of the goodness of fitting (R^2).

Table 3: Values of the Ci coefficients for the formula of *Staphylococcus aureus* (SA), *Pseudomonas aeruginosa* (PA) and *Klebsiella pneumonia* (KP)

Type of bacteria	C_1	C_2	C_3	C_4	C_5	C_6	R^2
SA	52961	-158808	-30221	-313144	7316	133536	1
PA	97145	-1177790	-380511	291595	592198	2110452	1
KP	-3105	-57128	-7017	-25398	9283	49805	1

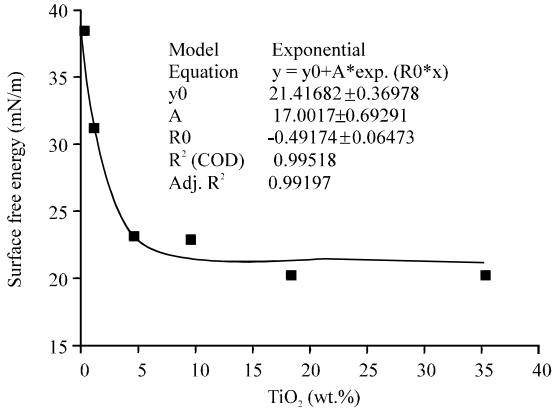

Fig. 10: The Surface Free Energy (SFE) of the TiO_2/PMMA composites

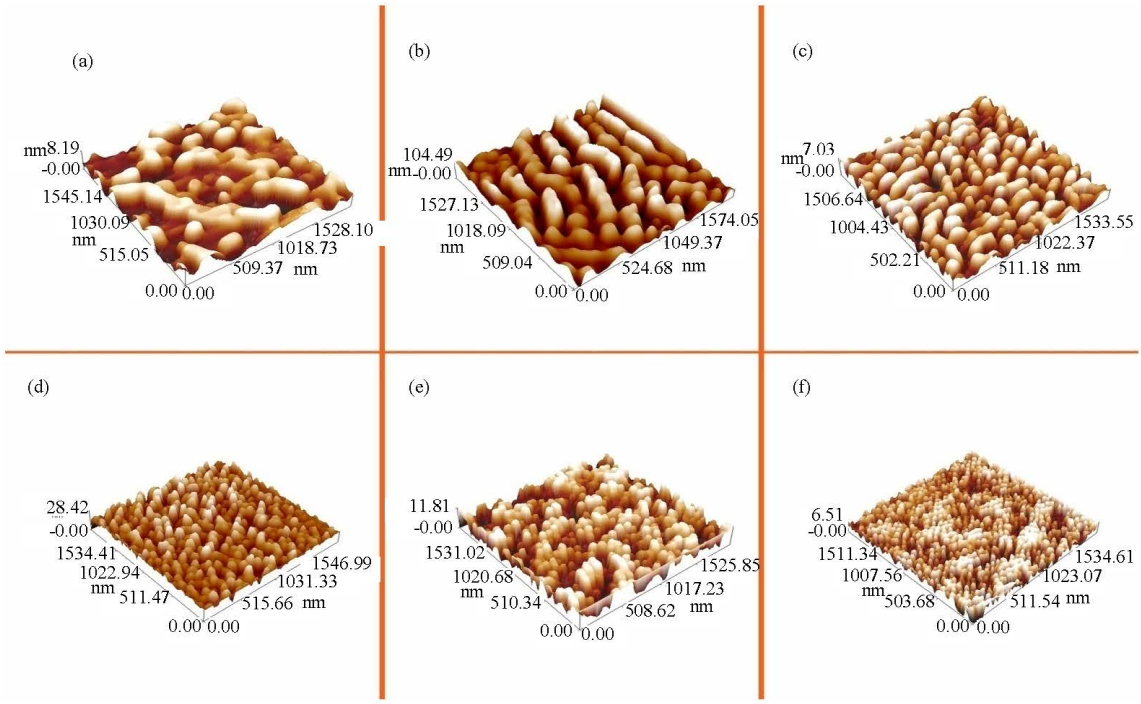

Fig. 11: The 3D nanoscale topographical images of surface of TiO_2/PMMA composites

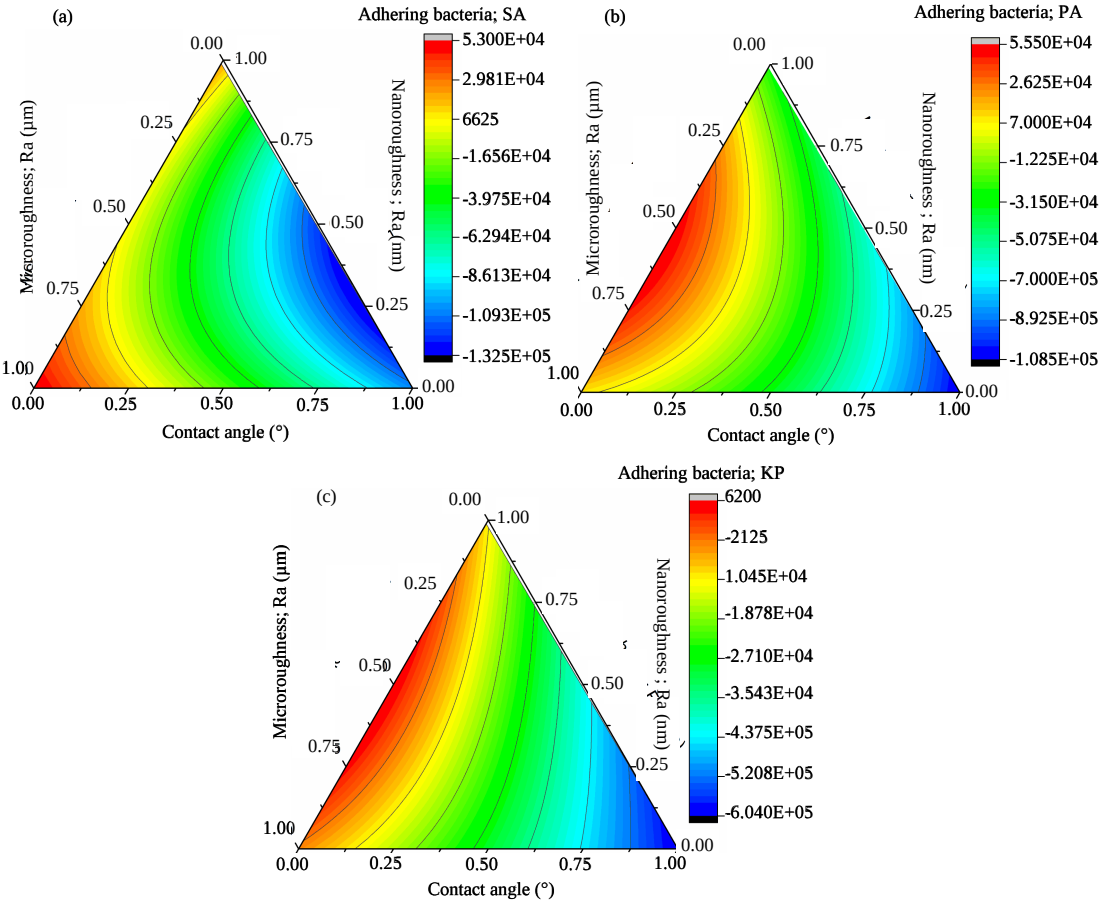

Fig. 12: The adhering behavior of the; a) *Staphylococcus aureus* (SA); b) *Pseudomonas aeruginosa* (PA) and c) *Klebsiella pneumonia* (KP)

In order to demonstratethe adhering of the selected bacterialspecies to the surfaces of the TiO_2/PMMA composites, ternary contour graphs have been adopted to represent the three selected independent variables. This type of graphs is used for the first time, for this purpose, in the current study. It can be seen that *Pseudomonas aeruginosa* (PA), *Staphylococcus aureus* (SA) and *Klebsiella pneumonia* (KP) prefer a surface with low to moderate contact angle, i.e., hydrophilic surface. This is because of the hydrophilic nature of the surfaces of these species (Al-Tahhan, 1998; Camprubi *et al*., 1992; Lerebour *et al*., 2004) that allow them to be attached largely to hydrophilic surfaces (Guegan *et al*., 2014; Al-Tahhan, 1998). Moreover, it has been found that TiO_2/PMMA composites with low nanoscale roughness aren't preferable for the adhesion of bacteria for all the selected bacterial species indicating that the low nanoscale topographical features play an important role in the resistance to bacterial adhesion. In the recent studies, it has been reported that these features trap air bubbles that form a barrier between the bacteria and the solid surface that prevents the bacteria to cross the air-water interface (Hasan *et al*., 2018; Belaabed *et al*., 2016). The microscale roughness, on the other hand is preferred by the selected species may be due to the compatibility of their sizes and shapes with the microscale features that helps them to anchor to the surface in agreement with the findings of recent report (Kathiresan and Mohan, 2017; Truong *et al*., 2010).

In order to compare the affinity of the selected species to the surface of the TiO_2/PMMA composites, a common axis for the dependent variable has been used in the ternary graphs to show their relative adhering as shown in Fig. 13. It is obvious that the sequence of the affinity of the species to adhere to the surface is *Klebsiella pneumonia*<*Staphylococcus aureus*<*Pseudomonas aeruginosa*. This sequence is in agreement with that reported in literatures (Gu and Ren, 2014; Barrett, 1988; Ahearn *et al*., 2000), this indicates the validity of the obtained models and the potential of the ternary contour graph to represent this kind of results.

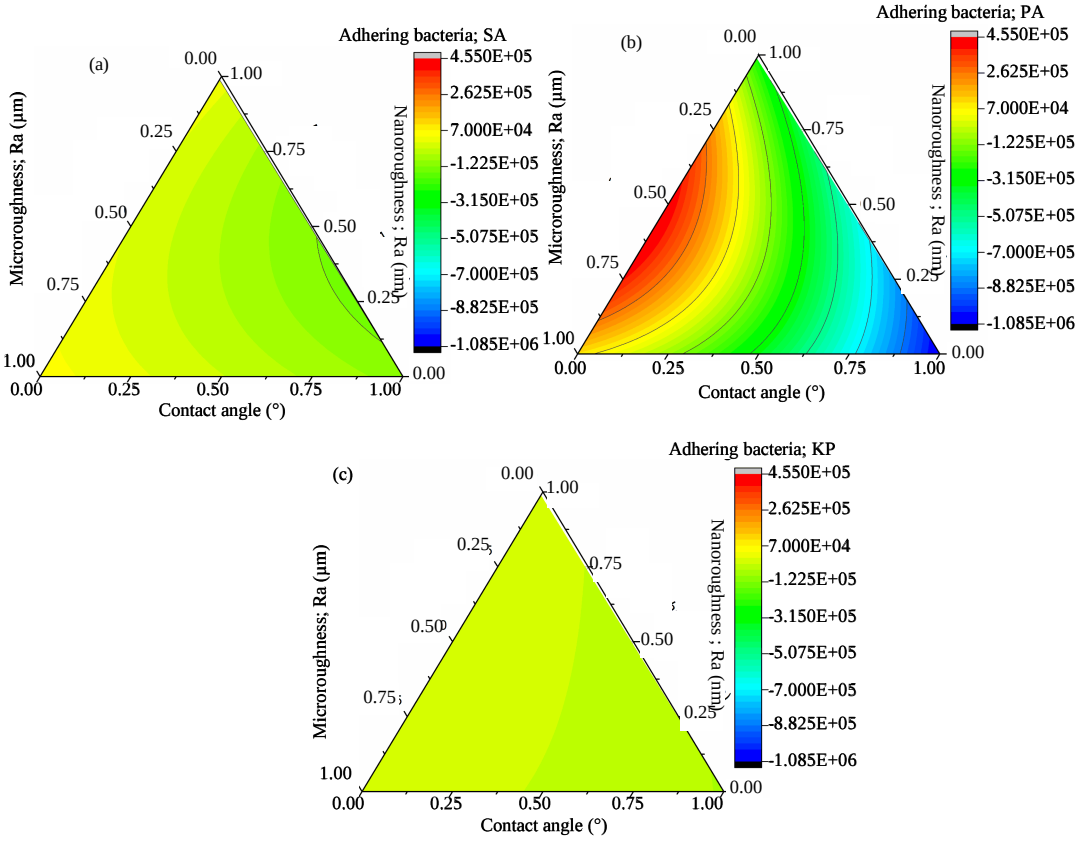

Fig. 13: A comparison among the adhesion of the; a) *Staphylococcus aureus* (SA); b) *Pseudomonas aeruginosa* (PA) and c) *Klebsiella pneumonia* (KP)

CONCLUSION

Incorporating the anatase nanoparticles into PMM Amatrix improves the stiffness, the hardness and the compressive strength of the composites, however, the bending strength is reduced when high loading percents of TiO_2 nanoparticles is used. Also, the surface features of the composites are highly affected by the addition of anatase nanoparticles in terms of contact angle, microscale roughness and the nanoscale roughness.

The maximum resistance to the adhesion of *Klebsiella pneumonia*, *Staphylococcus aureus* and *Pseudomonas aeruginosa* species can be achieved when the surface has high contact angle and low nanoscale roughness. The TiO_2/PMMA composite containing 10 wt.% of anatase nanoparticles compromises between the resistance to the adhesion of these species and the mechanical properties of the composite.

The number of the adhering bacteria can be correlated to the contact angle, nanoscale roughness and microscale roughness as independent variables using nonlinear regression technique. The regressions analysis produced a common model with different coefficients which is suitable to fit the adhesion data of the selected species that have different surface characteristics, size and shape; Namely the gram negative Coccobacillui bacteria (*Klebsiella pneumonia*), gram positive Cocci bacteria (*Staphylococcus aureus*) and the gram negative Bacilli bacteria (*Pseudomonas aeruginosa*).

REFERENCES

AL-Rubiae, M.S., 2016. Polymer-Nanoparticles composites for the reduction of the bacterial adherence to surfaces. Iraqi J. Biotechnol., 15: 17-24.

Ahearn, D.G., D.T. Grace, M.J. Jennings, R.N. Borazjani and K.J. Boles *et al*., 2000. Effects of hydrogel-silver coatings on *in vitro* adhesion to catheters of bacteria associated with urinary tract infections. Curr. Microbiol., 41: 120-125.

Al-Hydary, I.A.D., 2014. Preparation and characterization of phase-pure Anatase nanoparticles. Iraqi J. Mech. Mater. Eng., 14: 98-106.

Al-Tahhan, R.A.R., 1998. Cell surface hydrophobicity of *Pseudomonas aeruginosa*: Effects of monorhamnolipid and substrate on fatty acid and lipopolysaccharide content. Ph.D Thesis, University of Arizona, Tucson, Arizona.

An, Y.H. and R.J. Friedman, 1998. Concise review of mechanisms of bacterial adhesion to biomaterial surfaces. J. Biomed. Mater. Res., 43: 338-348.

Balamurugan, A., S. Kannan, V. Selvaraj and S. Rajeswari, 2004. Development and spectral characterization of poly (Methyl methacrylate)-hydroxyapatite composite for biomedical applications. Trends Biomater. Artif. Organs, 18: 41-45.

Barrett, S.P., 1988. Bacterial adhesion to intravenous cannulae: Influence of implantation in the rabbit and of enzyme treatments. Epidemiol. Infect., 100: 91-100.

Belaabed, R., S. Elabed, A. Addaou, A. Laajab and M.A. Rodriguez *et al*., 2016. Synthesis of LTA zeolite for bacterial adhesion. Bull. Spanish Soc. Ceram. Glass, 55: 152-158.

Busani, T. and R.A.B. Devine, 2005. Dielectric and infrared properties of TiO_2 films containing anatase and rutile. Semicond. Sci. Technol., 20: 870-875.

Camprubi, S., S. Merino, J. Benedi, P. Williams and J.M. Tomas, 1992. Physicochemical surface properties of *Klebsiella pneumoniae*. Curr. Microbiol., 24: 31-33.

Chaw, K.C., M. Manimaran and F.E. Tay, 2005. Role of silver ions in destabilization of intermolecular adhesion forces measured by atomic force microscopy in *Staphylococcus epidermidis* biofilms. Antimicrob. Agents Chemother., 49: 4853-4859.

Cheng, G., Z. Zhang, S. Chen, J.D. Bryers and S. Jiang, 2007. Inhibition of bacterial adhesion and biofilm formation on Zwitterionic surfaces. Biomater., 28: 4192-4199.

Crosby, A.J. and J.Y. Lee, 2007. Polymer nanocomposites: The nano effect on mechanical properties. Polym. Rev., 47: 217-229.

Donlan, R.M., 2002. Biofilms: Microbial life on surfaces. Emerg. Infect. Dis., 8: 881-890.

Furno, F., K.S. Morley, B. Wong, B.L. Sharp and P.L. Arnold *et al*., 2004. Silver nanoparticles and polymeric medical devices: A new approach to prevention of infection? J. Antimicrob. Chemother, 54: 1019-1024.

Giordano, C., E. Saino, L. Rimondini, M.P. Pedeferri and L. Visai *et al*., 2011. Electrochemically induced anatase inhibits bacterial colonization on Titanium Grade 2 and Ti6Al4V alloy for dental and orthopedic devices. Colloids Surf. B. Biointerfaces, 88: 648-655.

Gu, H. and D. Ren, 2014. Materials and surface engineering to control bacterial adhesion and biofilm formation: A review of recent advances. Front. Chem. Sci. Eng., 8: 20-33.

Gu, J., P.Z. Chen, B.B. Seo, J.M. Jardin and M.S. Verma *et al*., 2016. Adhesion characteristics of *Staphylococcus aureus* bacterial cells on funnel-shaped palladium-cobalt alloy nanostructures. J. Exp. Nanosci., 11: 480-489.

Guegan, C., J. Garderes, L.G. Pennec, F. Gaillard and F. Fay *et al*., 2014. Alteration of bacterial adhesion induced by the substrate stiffness. Colloids Surf. B. Biointerfaces, 114: 193-200.

Habash, M. and G. Reid, 1999. Microbial biofilms: Their development and significance for medical device-related infections. J. Clin. Pharmacol., 39: 887-898.

Habimana, O., A.J.C. Semiao and E. Casey, 2014. The role of cell-surface interactions in bacterial initial adhesion and consequent biofilm formation on nanofiltration/reverse osmosis membranes. J. Membr. Sci., 454: 82-96.

Han, A., J.K. Tsoi, F.P. Rodrigues, J.G. Leprince and W.M. Palin, 2016. Bacterial adhesion mechanisms on dental implant surfaces and the influencing factors. Intl. J. Adhes., 69: 58-71.

Hasan, J., S. Jain, R. Padmarajan, S. Purighalla and V.K. Sambandamurthy *et al*., 2018. Multi-scale surface topography to minimize adherence and viability of nosocomial drug-resistant bacteria. Mater. Des., 140: 332-344.

He, Z., Q. Cai, H. Fang, G. Situ and J. Qiu *et al*., 2013. Photocatalytic activity of TiO_2 containing anatase nanoparticles and rutile nanoflower structure consisting of nanorods. J. Environ. Sci., 25: 2460-2468.

Jiang, W., H. Mashayekhi and B. Xing, 2009. Bacterial toxicity comparison between nano-and micro-scaled oxide particles. Environ. Pollut., 157: 1619-1625.

Kathiresan, S. and B. Mohan, 2017. *In-vitro* bacterial adhesion study on stainless steel 316L subjected to magneto rheological abrasive flow finishing. Biomed. Res., 28: 3169-3175.

Lerebour, G., S. Cupferman and M.N. Bellon-Fontaine, 2004. Adhesion of *Staphylococcus aureus* and *Staphylococcus epidermidis* to the Episkin® reconstructed epidermis model and to an inert 304 stainless steel substrate. J. Appl. Microbiol., 97: 7-16.

Li, B. and B.E. Logan, 2004. Bacterial adhesion to glass and metal-oxide surfaces. Colloids Surf. B. Biointerfaces, 36: 81-90.

Li, B. and Q. Ye, 2015. Antifouling Surfaces of Self-Assembled Thin Layer. In: Antifouling Surfaces and Materials, Zhou, F. (Ed.). Springer, Berlin, Germany, ISBN:978-3-662-45203-5, pp: 31-54.

Lipschitz, I., 1982. The vibrational spectrum of poly (Methyl methacrylate): A review. Polym. Plast. Technol. Eng., 19: 53-106.

Lorenzetti, M., I. Dogsa, T. Stosicki, D. Stopar and M. Kalin *et al*., 2015. The influence of surface modification on bacterial adhesion to titanium-based substrates. ACS. Appl. Mater. Interfaces, 7: 1644-1651.

Nakamoto, K., 2009. Infrared and Raman Spectra of Inorganic and Coordination Compounds: Theory and Applications in Inorganic Chemistry. 6th Edn., John Wiley and Sons, USA., pp: 419.

Pavithra, D. and M. Doble, 2008. Biofilm formation, bacterial adhesion and host response on polymeric implants-issues and prevention. Biomed. Mater., 3: 1-13.

Puckett, S.D., E. Taylor, T. Raimondo and T.J. Webster, 2010. The relationship between the nanostructure of titanium surfaces and bacterial attachment. Biomaterials, 31: 706-713.

Quirynen, M., M. Marechal, H.J. Busscher, A.H. Weerkamp and P.L. Darius *et al*., 1990. The influence of surface free energy and surface roughness on early plaque formation: An in vivo study in man. J. Clin. Periodontology, 17: 138-144.

Razatos, A., Y.L. Ong, M.M. Sharma and G. Georgiou, 1998. Molecular determinants of bacterial adhesion monitored by atomic force microscopy. Proc. Nat. Acad. Sci., 95: 11059-11064.

Rochford, E.T.J., A.H.C. Poulsson, J.S. Varela, P. Lezuo and R.G. Richards *et al*., 2014. Bacterial adhesion to orthopaedic implant materials and a novel oxygen plasma modified PEEK surface. Colloids Surf. B. Biointerfaces, 113: 213-222.

Rodrigues, L.R., 2011. Inhibition of Bacterial Adhesion on Medical Devices. In: Bacterial Adhesion, Linke, D. and A. Goldman (Eds.). Springer, Dordrecht, Netherlands, ISBN:978-94-007-0939-3, pp: 351-367.

Schaechter, M., 2004. The Desk Encyclopedia of Microbiology. 1st Edn., Elsevier Academic Press, New York.

Sharmila, G., S. Haries, M.F. Fathima, S. Geetha and N.M. Kumar *et al*., 2017. Enhanced catalytic and antibacterial activities of phytosynthesized palladium nanoparticles using *Santalum album* leaf extract. Powder Technol., 320: 22-26.

Singh, A., A. Ahmed, K.N. Prasad, S. Khanduja and S.K. Singh *et al*., 2015. Antibiofilm and membrane-damaging potential of cuprous oxide nanoparticles against *Staphylococcus aureus* with reduced susceptibility to vancomycin. Antimicrob. Agents Chemother., 59: 6882-6890.

Song, F., H. Koo and D. Ren, 2015. Effects of material properties on bacterial adhesion and biofilm formation. J. Dent. Res., 94: 1027-1034.

Speranza, G., G. Gottardi, C. Pederzolli, L. Lunelli and R. Canteri *et al*., 2004. Role of chemical interactions in Bacterial adhesion to polymer surfaces. Biomater., 25: 2029-2037.

Tanner, J., C. Robinson, E. Soderling and P. Vallittu, 2005. Early plaque formation on fibre-reinforced composites *In vivo*. Clin. Oral Invest., 9: 154-160.

Teughels, W., V.N. Assche, I. Sliepen and M. Quirynen, 2006. Effect of material characteristics and-or surface topography on biofilm development. Clin. Oral Implants Res., 17: 68-81.

Torres, A.G., C. Jeter, W. Langley and A.G. Matthysse, 2005. Differential binding of *Escherichia coli* O157: H7 to alfalfa, human epithelial cells and plastic is mediated by a variety of surface structures. Appl. Environ. Microbiol., 71: 8008-8015.

Truong, V.K., R. Lapovok, Y.S. Estrin, S. Rundell and J.Y. Wang *et al*., 2010. The influence of nano-scale surface roughness on bacterial adhesion to ultrafine-grained titanium. Biomaterials, 31: 3674-3683.

Wassmann, T., S. Kreis, M. Behr and R. Buergers, 2017. The influence of surface texture and wettability on initial bacterial adhesion on titanium and Zirconium oxide dental implants. Intl. J. Implant Dent., 3: 1-11.

Xing, S.F., X.F. Sun, A.A. Taylor, S.L. Walker and Y.F. Wang *et al*., 2015. D-Amino acids inhibit initial bacterial Adhesion: Thermodynamic evidence. Biotechnol. Bioeng., 112: 696-704.

Zhang, X., L. Wang and E. Levanen, 2013. Superhydrophobic surfaces for the reduction of bacterial adhesion. Rsc. Adv., 3: 12003-12020.